Available online at www.sciencedirect.com

ScienceDirect

Nuclear Physics B 898 (2015) 644–658

NUCLEAR PHYSICS B

www.elsevier.com/locate/nuclphysb

The supersymmetric Higgs boson with flavoured A-terms

Andrea Brignole

INFN, Sezione di Padova, via Marzolo 8, I-35131 Padova, Italy

Received 24 April 2015; received in revised form 11 July 2015; accepted 21 July 2015

Available online 28 July 2015

Editor: Tommy Ohlsson

Abstract

We consider a supersymmetric scenario with large flavour violating A-terms in the stop/scharm sector and study their impact on the Higgs mass, the electroweak ρ parameter and the effective Higgs couplings to gluons, photons and charm quarks. For each observable we present explicit analytical expressions which exhibit the relevant parametric dependences, both in the general case and in specific limits. We find significant effects and comment on phenomenological implications for the LHC and future colliders.

1. Introduction

The recent discovery of a Higgs particle at the LHC [1] has confirmed the validity of the Standard Model (SM). ATLAS and CMS have found that the Higgs boson has a mass of 125 GeV [2] and that its couplings to gauge bosons and third-generation fermions are consistent with the SM predictions [3,4]. The experimental uncertainties on Higgs couplings are still sizable, but they will be progressively reduced, first at the LHC and then at future colliders. Several models of physics beyond the SM will be tested as well, since they generically predict both deviations in those couplings and new particles to be discovered. Supersymmetric (SUSY) extensions of the SM are well known examples of such theories. In a wide class of SUSY models, including the MSSM and the NMSSM, the Higgs sector contains two doublets and possibly singlets [5–7].

E-mail address: brignole@pd.infn.it.

http://dx.doi.org/10.1016/j.nuclphysb.2015.07.025

A linear combination of the doublets ($H = \sin\beta\, H_u - \cos\beta\, i\sigma_2 H_d^*$) behaves as the SM doublet in the decoupling limit of the other Higgs states. We will focus on this regime for definiteness. Our aim is to investigate some properties of such SM-like Higgs field in a particular region of the SUSY parameter space, characterized by large values of certain flavour violating trilinear couplings.

Let us parametrize the neutral component of H as $H^0 = v + \frac{1}{\sqrt{2}}(h + iG)$, where $v \simeq 174$ GeV triggers $SU(2) \times U(1)$ breaking, h is the physical Higgs boson and G is the neutral would-be Goldstone boson. Stop squarks are the SUSY particles that couple more strongly to H^0. Indeed, F-terms generate large quartic couplings of the form $y_t^2|H^0|^2(|\tilde{t}_L|^2 + |\tilde{t}_R|^2)$, where y_t is the SM top Yukawa coupling (*i.e.*, y_t is related to the top mass through $m_t = y_t\, v$ at the tree level). F-terms and SUSY-breaking A-terms also generate Higgs-stop-stop trilinear couplings. We assume that sizable Higgs-stop-scharm A-terms are present as well, although we do not specify their origin. Hence the trilinear scalar interactions that are relevant to us are

$$V_{(3)} = y_t\, H^0\, (X_t\, \tilde{t}_R^*\, \tilde{t}_L + A_{tc}\, \tilde{t}_R^*\, \tilde{c}_L + A_{ct}\, \tilde{c}_R^*\, \tilde{t}_L) + \text{h.c.}\,, \tag{1}$$

where we have used the standard notation $X_t \equiv A_t - \mu^* \cot\beta$ and factored out y_t for convenience. We complete our parametrization by writing stop and scharm (SUSY-breaking) mass terms as $\tilde{m}_{t_L}^2|\tilde{t}_L|^2 + \tilde{m}_{t_R}^2|\tilde{t}_R|^2 + \tilde{m}_{c_L}^2|\tilde{c}_L|^2 + \tilde{m}_{c_R}^2|\tilde{c}_R|^2$. Gauge invariance implies mass terms $\tilde{m}_{t_L}^2|\tilde{b}_L|^2 + \tilde{m}_{c_L}^2|\tilde{s}_L|^2$ for $\tilde{b}_L$ and $\tilde{s}_L$, the $SU(2)$ partners of $\tilde{t}_L$ and $\tilde{c}_L$. In general one also expects flavour violating mass terms of LL and RR type, as well as other LR trilinears. The effective low-energy values of all such parameters depend, as usual, both on boundary conditions at some higher scale and on renormalization effects, which include those generated by A_{tc} and A_{ct} themselves. Although we are aware of the latter connection, we decide to explore the region of the phenomenological SUSY parameter space where all flavour violating masses are small, apart from those in eq. (1). In other words, we do not specify either a flavour model or a mechanism of SUSY breaking, treat A_{tc} and A_{ct} as phenomenological parameters (on the same footing as X_t) and allow them to be as large as the flavour conserving stop and scharm masses. Even in the latter limit the constraints from flavour changing observables are weak or absent, especially for $\mathcal{O}$(TeV) squark masses. We will return to this point in a separate paper [8], whereas here we will study the impact of A_{tc} and A_{ct} on a set of *flavour conserving* quantities, namely:

i) the mass of the Higgs boson h (Section 2);
ii) the ρ parameter (Section 3);
iii) the effective coupling of h to gluons or photons (Section 4);
iv) the effective coupling of h to charm quarks (Section 5).

In each case we will compute the leading effects and present simple analytical expressions which exhibit the relevant parametric dependences. By 'leading' we mean that squarks are integrated out at the one-loop level, at leading order in y_t and at lowest order in $v^2/\tilde{m}^2$, where $\tilde{m}^2$ generically denotes a squark mass. In the effective theory language, the latter point means that we evaluate the squark contribution to the operators of lowest dimension (d) associated with each of the above quantities, namely:

i) $|H^0|^4$ ($d = 4$);
ii) $|H^\dagger D_\mu H|^2$ ($d = 6$);
iii) $|H^0|^2 G_{\mu\nu} G^{\mu\nu}$, $|H^0|^2 F_{\mu\nu} F^{\mu\nu}$ ($d = 6$);
iv) $|H^0|^2 H^0\, \overline{c_R}\, c_L + \text{h.c.}$ ($d = 6$).

These different dimensionalities imply different decoupling properties, of course. Squark contributions to ρ and to the effective Higgs couplings are suppressed by a factor $v^2/\tilde{m}^2$ ($d = 6$ operators). On the other hand, corrections to the Higgs mass do not feel that suppression since they are associated to a quartic coupling ($d = 4$ operator). In any case, once the appropriate power of $v^2/\tilde{m}^2$ is taken into account, for each of the above quantities the remaining dependence on mass parameters will be encoded in some dimensionless function. In particular, the dependence on trilinear parameters will appear through powers of $X_t/\tilde{m}$, $A_{tc}/\tilde{m}$, $A_{ct}/\tilde{m}$.

2. The Higgs mass

In the SM the Higgs mass is $m_h^2 = \lambda v^2$ at the tree level, where λ is a free parameter that controls the quartic term of the Higgs potential ($V \supset \frac{1}{4}\lambda|H^0|^4$). The measured value of $m_h \simeq 125$ GeV implies $\lambda \simeq 0.5$ at the weak scale. In SUSY scenarios with a SM-like Higgs, λ is an effective coupling that can receive contributions from different sources: $\lambda \simeq \sum_i \delta\lambda_i$. At the tree level the standard D-term contribution $\delta\lambda_D = \frac{1}{2}(g^2 + g'^2)\cos^2 2\beta$ predicts $m_h = m_Z|\cos 2\beta| \leq m_Z$, significantly lower than 125 GeV. Additional tree-level contributions to λ can arise, *e.g.*, from F-terms in extensions with singlets [7] or from higher dimension effective operators [9]. Important contributions to λ also arise radiatively. The leading ones are generated by top and stop one-loop diagrams [10] and are proportional to y_t^4:

$$\delta\lambda_{\log} \simeq \frac{3y_t^4}{4\pi^2}\log\frac{\tilde{m}_t^2}{m_t^2}, \quad \delta\lambda_{\rm thr} \simeq \frac{3y_t^4}{4\pi^2}\Delta\,. \tag{2}$$

The first term $\delta\lambda_{\log}$ can be interpreted either as the combination of logarithmically divergent top and stop contributions, or as the result of the top-loop-induced running of λ from the stop mass scale $\tilde{m}_t^2 \simeq (\tilde{m}_{t_L}^2\tilde{m}_{t_R}^2)^{1/2}$ to the weak scale ($4\pi^2 d\lambda/d\log q^2 = -3y_t^4 + \cdots$). The second term $\delta\lambda_{\rm thr}$ is a finite threshold correction at the stop scale and we parametrize it through Δ, a dimensionless function of squark mass parameters.[1] In the flavour conserving limit, Δ contains quadratic and quartic powers of X_t. As well known, an appropriate choice of X_t can give a substantial contribution to Δ, which translates into a correction $\delta m_h^2 \simeq \delta\lambda_{\rm thr} v^2$ to the Higgs mass. In the often quoted limit $\tilde{m}_{t_L}^2 = \tilde{m}_{t_R}^2 = \tilde{m}_t^2$, for instance, $\Delta = |X_t|^2/\tilde{m}_t^2 - \frac{1}{12}|X_t|^4/\tilde{m}_t^4$ reaches its maximal value $\Delta_{\max} = 3$ at $|X_t| = \sqrt{6}\tilde{m}_t$. The corresponding linear correction to m_h is about 15–20 GeV. We recall that, as often emphasized, a large threshold correction is welcome because it allows a smaller stop mass scale in the logarithmic term (*e.g.*, $\tilde{m}_t$ around 1 TeV rather than in the multi-TeV range). However, the knowledge of the threshold correction is important also in more general scenarios.

Our purpose in this section is to generalize the one-loop calculation of Δ by including the effect of the flavour violating A-terms A_{tc} and A_{ct} of eq. (1), which couple the Higgs field to stop and scharm squarks. The one-loop stop/scharm diagrams that contribute to Δ at $\mathcal{O}(y_t^4)$ are shown in Fig. 1. Those in the first (second) row are quadratic (quartic) in X_t, A_{tc}, A_{ct} and give

[1] More precisely, the tree-level contributions and $\delta\lambda_{\rm thr}$ determine the SM coupling λ at the SUSY matching scale. The latter coupling is then renormalized down to the weak scale where m_h is evaluated. For recent investigations on the SUSY threshold effect, RG evolution and higher order corrections, see [11] and refs. therein. If one uses the approximate expressions in eq. (2), the factors y_t^4 may be evaluated at the scales suggested in [12], *i.e.* at $(m_t\tilde{m}_t)^{1/2}$ in $\delta\lambda_{\log}$ and at $\tilde{m}_t$ in $\delta\lambda_{\rm thr}$.

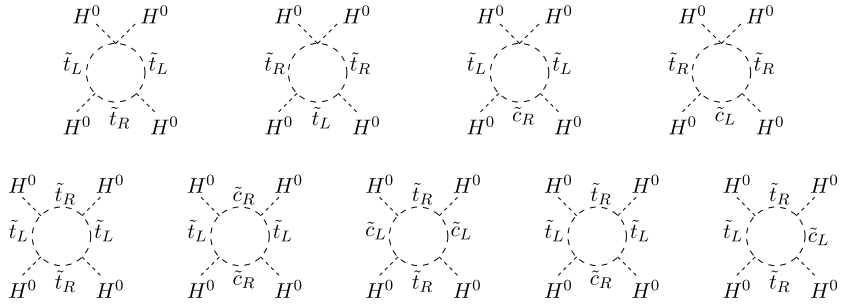

Fig. 1. One-loop stop/scharm diagrams that contribute to the Higgs quartic coupling at $\mathcal{O}(y_t^4)$ through trilinear interactions.

positive (negative) contributions to Δ. We find:

$$\begin{aligned}\Delta = {} & \frac{|X_t|^2}{\tilde{m}_{t_L}^2 - \tilde{m}_{t_R}^2} \log \frac{\tilde{m}_{t_L}^2}{\tilde{m}_{t_R}^2} + \frac{|A_{ct}|^2}{\tilde{m}_{c_R}^2} f_1\left(\frac{\tilde{m}_{t_L}^2}{\tilde{m}_{c_R}^2}\right) + \frac{|A_{tc}|^2}{\tilde{m}_{c_L}^2} f_1\left(\frac{\tilde{m}_{t_R}^2}{\tilde{m}_{c_L}^2}\right) \\ & - \frac{1}{2}\left[\frac{|X_t|^4}{\tilde{m}_{t_L}^4} f_2\left(\frac{\tilde{m}_{t_R}^2}{\tilde{m}_{t_L}^2}\right) + \frac{|A_{ct}|^4}{\tilde{m}_{c_R}^4} f_2\left(\frac{\tilde{m}_{t_L}^2}{\tilde{m}_{c_R}^2}\right) + \frac{|A_{tc}|^4}{\tilde{m}_{c_L}^4} f_2\left(\frac{\tilde{m}_{t_R}^2}{\tilde{m}_{c_L}^2}\right)\right] \\ & - \frac{|X_t|^2 |A_{ct}|^2}{\tilde{m}_{c_R}^2 - \tilde{m}_{t_R}^2}\left[\frac{1}{\tilde{m}_{t_R}^2} f_1\left(\frac{\tilde{m}_{t_L}^2}{\tilde{m}_{t_R}^2}\right) - \frac{1}{\tilde{m}_{c_R}^2} f_1\left(\frac{\tilde{m}_{t_L}^2}{\tilde{m}_{c_R}^2}\right)\right] \\ & - \frac{|X_t|^2 |A_{tc}|^2}{\tilde{m}_{c_L}^2 - \tilde{m}_{t_L}^2}\left[\frac{1}{\tilde{m}_{t_L}^2} f_1\left(\frac{\tilde{m}_{t_R}^2}{\tilde{m}_{t_L}^2}\right) - \frac{1}{\tilde{m}_{c_L}^2} f_1\left(\frac{\tilde{m}_{t_R}^2}{\tilde{m}_{c_L}^2}\right)\right], \end{aligned} \tag{3}$$

where $f_i(x)$ are positive functions [with $f_1(1) = \frac{1}{2}$, $f_2(1) = \frac{1}{6}$]:

$$f_1(x) = -\frac{1}{(x-1)^2}\log x + \frac{1}{x-1}, \quad f_2(x) = \frac{x+1}{(x-1)^3}\log x - \frac{2}{(x-1)^2}. \tag{4}$$

The overall size of the threshold function Δ as well as its sign depend on the competition of positive and negative terms, in analogy to the familiar case with X_t only. The novel contributions induced by A_{ct} and A_{tc} can be of the same order as the standard ones driven by X_t. As the total effect depends on several mass parameters, a pre-fixed value of Δ is associated with some hypersurface in a multi-dimensional parameter space. To simplify the discussion, suppose that $(\tilde{t}_L, \tilde{t}_R)$ have a common mass $\tilde{m}_t^2$ ($\simeq \tilde{m}_{t_L}^2 \simeq \tilde{m}_{t_R}^2$) and that $(\tilde{c}_L, \tilde{c}_R)$ have a common mass $\tilde{m}_c^2$ ($\simeq \tilde{m}_{c_L}^2 \simeq \tilde{m}_{c_R}^2$). In this limit, the threshold function becomes:

$$\begin{aligned}\Delta = {} & \frac{|X_t|^2}{\tilde{m}_t^2} + \frac{|A_{ct}|^2 + |A_{tc}|^2}{\tilde{m}_c^2} f_1\left(\frac{\tilde{m}_t^2}{\tilde{m}_c^2}\right) - \left[\frac{1}{12}\frac{|X_t|^4}{\tilde{m}_t^4} + \frac{1}{2}\frac{|A_{ct}|^4 + |A_{tc}|^4}{\tilde{m}_c^4} f_2\left(\frac{\tilde{m}_t^2}{\tilde{m}_c^2}\right)\right. \\ & \left. + \frac{|X_t|^2}{\tilde{m}_t^2} \cdot \frac{|A_{ct}|^2 + |A_{tc}|^2}{\tilde{m}_c^2} f_3\left(\frac{\tilde{m}_t^2}{\tilde{m}_c^2}\right)\right], \end{aligned} \tag{5}$$

where $f_3(x)$ is another positive function [with $f_3(1) = \frac{1}{6}$]:

$$f_3(x) = -\frac{x}{(x-1)^3}\log x + \frac{x+1}{2(x-1)^2}. \tag{6}$$

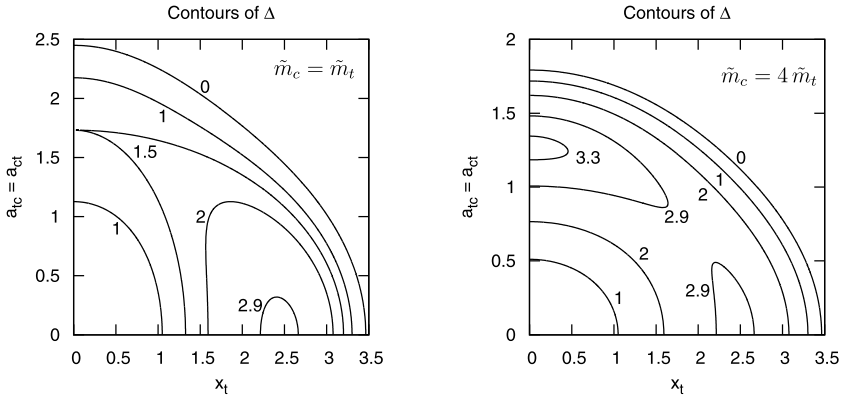

Fig. 2. Iso-contours of Δ in the subspace spanned by x_t and $a_{tc} = a_{ct}$, for $r = 1$ ($\tilde{m}_c = \tilde{m}_t$, left panel) and $r = 4$ ($\tilde{m}_c = 4\,\tilde{m}_t$, right panel).

A further simplification occurs in the fully degenerate limit $\tilde{m}_c^2 = \tilde{m}_t^2 = \tilde{m}^2$:

$$\Delta = \frac{|X_t|^2}{\tilde{m}^2} + \frac{|A_{tc}|^2 + |A_{ct}|^2}{2\tilde{m}^2} - \frac{|X_t|^4 + |A_{tc}|^4 + |A_{ct}|^4 + 2|X_t|^2(|A_{tc}|^2 + |A_{ct}|^2)}{12\,\tilde{m}^4}\,. \tag{7}$$

Let us consider, for instance, the simplified expression in eq. (7). Here Δ is a function of only three dimensionless variables, namely $(x_t, a_{tc}, a_{ct}) \equiv (|X_t|/\tilde{m}, |A_{tc}|/\tilde{m}, |A_{ct}|/\tilde{m})$. By a simple analytical study, we find the interesting result that Δ is maximal at the 'standard point' $(x_t, a_{tc}, a_{ct}) = (\sqrt{6}, 0, 0)$, where $\Delta = 3$. There are other extremal points where the flavour changing trilinears do not vanish, namely $(0, \sqrt{3}, 0)$, $(0, 0, \sqrt{3})$ and $(0, \sqrt{3}, \sqrt{3})$. At such extrema, which are saddle points, Δ take values 3/4, 3/4 and 3/2, respectively. In a significant portion of the three-dimensional parameter space spanned by (x_t, a_{tc}, a_{ct}) one can obtain $\Delta \gtrsim 1$. The role of x_t is crucial in order to reach $\Delta \gtrsim 2$.

Consider now a slightly more general scenario in which stop and scharm masses are characterized by two distinct parameters $\tilde{m}_t^2$ and $\tilde{m}_c^2$, such that Δ is given by eq. (5). The parameter space can be described by three coordinates associated with the trilinear couplings, which we take as $(x_t, a_{tc}, a_{ct}) \equiv (|X_t|/\tilde{m}_t, |A_{tc}|/\tilde{m}_c, |A_{ct}|/\tilde{m}_c)$, plus the ratio $r \equiv \tilde{m}_c/\tilde{m}_t$, which we treat as an external parameter. By an analytical study of Δ for fixed r, we find the standard extremum at $(\sqrt{6}, 0, 0)$ as well as other ones at $(0, a_*, 0)$, $(0, 0, a_*)$ and $(0, a_*, a_*)$, where $a_* = \sqrt{f_1/f_2}$ and $f_i \equiv f_i(1/r^2)$. Another extremum (a saddle point) appears for $1 < r \lesssim 5$. The extremum at $(0, a_*, a_*)$ is interesting because it is a local maximum for $r > 1$. The associated value of Δ is $\Delta_* = f_1^2/f_2$, which increases for increasing r: for $r = (0.5;\ 1;\ 2;\ 3;\ 4;\ 5;\ 6)$ one finds $\Delta_* \simeq (0.9;\ 1.5;\ 2.3;\ 2.9;\ 3.4;\ 3.7;\ 4)$. This behaviour follows from the mild (logarithmic) enhancement of the coefficient functions f_1 and f_2, which is easily interpreted through the diagrams in Fig. 1. The other extrema $(0, a_*, 0)$ and $(0, 0, a_*)$ are saddle points and have $\Delta = \frac{1}{2}\Delta_*$. By comparing the reported values of Δ_* with $\Delta = 3$ at the standard extremum $(\sqrt{6}, 0, 0)$, we can see that the latter point is no longer the absolute maximum for $r \gtrsim 3$. For $r \gtrsim 5$, it is not even a local maximum and becomes a saddle point (namely, Δ increases if ones moves away from that point in the flavour violating directions).

The behaviour of the threshold function Δ is further illustrated in Fig. 2, where some iso-contours are shown in a two-dimensional subspace spanned by x_t and $a_{tc} = a_{ct}$, for either $r = 1$ (left panel) or $r = 4$ (right panel). The case $r = 1$ (namely, $\tilde{m}_c = \tilde{m}_t$) is the degenerate limit,

already discussed above. One can easily recognize the standard maximum at $x_t = \sqrt{6}$ (and $a_{tc} = a_{ct} = 0$), where $\Delta = 3$, and the other extremum (saddle point) at $a_{tc} = a_{ct} = \sqrt{3}$ (and $x_t = 0$), where $\Delta = 1.5$. The case $r = 4$ (namely, $\tilde{m}_c = 4\tilde{m}_t$) is an example of a moderately hierarchical scenario. The extremum on the $a_{tc} = a_{ct}$ axis has turned into a maximum, and Δ is higher there than at the standard maximum on the x_t axis. More generally, by comparing this case with the previous one, one can notice the expansion of the region of parameter space where $\Delta \gtrsim 2$, which translates into a linear correction to m_h larger than about 10 GeV. As $\Delta \gtrsim 3$ can also be obtained in such hierarchical scenarios, even shifts of $\mathcal{O}(20)$ GeV are possible. In summary, significant positive threshold corrections to the Higgs mass can be achieved in a variety of ways, by suitable combinations of the flavour conserving and flavour violating trilinear couplings. If any of such parameters is too large, though, the corrections quickly become negative, since Δ is then dominated by negative quartic terms. In our examples in Fig. 2 this occurs to the right of the iso-contours where $\Delta = 0$. Such parameter regions are also disfavoured because the tree-level potential can become unbounded from below along coloured directions or develop colour-breaking minima [13,14].

A side remark may be added about the impact of sizable values of A_{tc} and/or A_{ct} on the naturalness of the weak scale. In fact, although we have chosen to avoid discussing renormalization effects above the SUSY scale, it should be mentioned that the soft mass of the Higgs doublet H_u, *i.e.* $\tilde{m}^2_{H_u}$, receives logarithmic corrections proportional to $|A_t|^2 + |A_{tc}|^2 + |A_{ct}|^2$. Therefore fine-tuning issues are not alleviated by the presence of A_{tc} and A_{ct}, particularly in case such parameters are of order $\tilde{m}_c$ and the latter is much larger than $\tilde{m}_t$.

We conclude this section by some comments on earlier results presented in the literature. The influence of flavour violating A-terms on m_h was noticed in [15] and confirmed in [16]. However, such papers put a special emphasis on the potentially large *negative* effect of such trilinear couplings on the Higgs mass, which in fact was used to constrain their magnitude. On the other hand, it was recently pointed out in [17] that a sizable *positive* effect on m_h can also be achieved, especially in the case of a hierarchical squark spectrum ($\tilde{m}_c^2 \gg \tilde{m}_t^2$, in our notation). Our study confirms this observation. Upon comparing our analytical results with those presented in [17], though, we have found agreement only in the degenerate case [$\tilde{m}_c^2 = \tilde{m}_t^2$, eq. (7)], not in the non-degenerate one [$\tilde{m}_c^2 \neq \tilde{m}_t^2$, eq. (5)].

3. The ρ parameter

In the previous section we have examined certain SUSY corrections to the quartic operator $|H^0|^4$, which controls the mass of the physical Higgs boson $h \subset H^0$. Other properties of h will be investigated in subsequent sections. Here, instead, we will discuss the impact of SUSY corrections to the ρ parameter, where only the expectation value $\langle |H^0| \rangle = v$ is relevant. We select $\delta\rho$ ($= \epsilon_1 = \alpha\,\delta T$) as the most representative quantity that affects electroweak precision observables, and recall that new physics contributions to $\delta\rho$ are constrained to be at the per mille level at most [18]. For instance, $\delta\rho$ corrects the SM predictions for the W mass m_W^2 and the effective leptonic weak mixing angle $\sin^2\theta^\ell_{\rm eff}$ by an amount $\delta m_W^2/m_W^2 \simeq -\delta \sin^2\theta^\ell_{\rm eff}/s_w^2 \simeq a\,\delta\rho$, where $s_w^2 \simeq 0.23$ and $a = c_w^2/(c_w^2 - s_w^2) \simeq 1.4$. In particular, a positive $\delta\rho \simeq 10^{-3}$ would induce $\delta m_W \simeq 60$ MeV. This can be taken as a maximal allowed shift, since the current deviation on m_W is $m_W^{\rm SM} - m_W^{\rm exp} \simeq -25$ MeV, with a one-sigma error of about 17 MeV. More stringent constraints on $\delta\rho$ are expected from future measurements at the LHC and at other proposed colliders. For general new physics, a full analysis should include other possible sources of corrections to m_W^2 and $\sin^2\theta^\ell_{\rm eff}$, such as the S parameter. In our case, though, these effects are

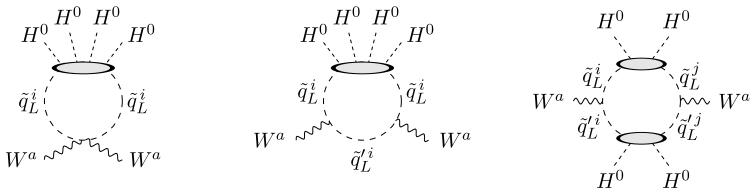

Fig. 3. Classes of one-loop squark diagrams that contribute to the self-energies of $SU(2)$ vector bosons with four Higgs insertions. The ovals indicate that Higgs lines can be inserted in all possible ways on squark propagators, through trilinear or quartic couplings. Only diagrams of the third class contribute to $\delta\rho$.

subleading (they are at most $\mathcal{O}(g^2 y_t^2)$, therefore smaller than the $\mathcal{O}(y_t^4)$ effects associated with $\delta\rho$).

Squark contributions to $\delta\rho$ can be evaluated through $\delta\rho = [\Pi_{33}(0) - \Pi_{WW}(0)]/m_W^2$, where $\Pi_{33}(0)$ and $\Pi_{WW}(0)$ are the self-energies of W^3 and $W^\pm$ at zero momentum (up to the usual factor $g_{\mu\nu}$). Diagrammatic computations have often been performed by diagonalizing the squark mass matrices and keeping the full dependence on v [19–21]. As already declared, we choose to evaluate diagrams by explicitly inserting Higgs lines and looking for the leading non-vanishing terms in a v^2 expansion. At $\mathcal{O}(v^0)$, both $\Pi_{33}(0)$ and $\Pi_{WW}(0)$ separately vanish by gauge invariance. At $\mathcal{O}(v^2)$, those self-energies receive equal contributions, so there is no net $\delta\rho$ at this order. The leading contributions to $\delta\rho$ arise from $\mathcal{O}(v^4)$ terms in W^a self-energies, so $\delta\rho \sim v^2/\tilde{m}^2$. In fact, as well known, such corrections are associated with the $d = 6$ effective operator $|H^\dagger D_\mu H|^2$: if c_ρ is the coefficient of the latter, $\delta\rho \simeq -c_\rho v^2$. As the relevant W^a self-energies require (at least) four Higgs insertions, we find it very convenient to group the one-loop squark diagrams that contribute to them into three classes, as shown schematically in Fig. 3. The symbols $\tilde{q}_L^i, \tilde{q}_L'^i$ generically denote up-type or down-type squarks of the i-th left-handed doublet, so it is understood that $\tilde{q}_L^i$ and $\tilde{q}_L'^i$ are equal (different) if they couple to W^3 ($W^\pm$). It is both useful and not restrictive to consider a basis where the 3×3 mass matrix $\tilde{m}_Q^2$ of $SU(2)$ doublets is diagonal, so flavour transitions can only occur at Higgs vertices or in $\tilde{q}_R$ propagators. Consider the first class of diagrams in Fig. 3. Each bilinear $|\tilde{q}_L^i|^2$ has the same quartic coupling to $|W^\pm|^2$ and to $\frac{1}{2}(W^3)^2$, by $SU(2)$ invariance. This implies that there are equal contributions to $\Pi_{33}(0)$ and $\Pi_{WW}(0)$, so the net contribution to $\delta\rho$ is zero. A similar argument can be applied to the second class of diagrams. Again, the $SU(2)$ properties of the W^a–$\tilde{q}_L^i$–$\tilde{q}_L'^i$ vertices imply equal contributions to $\Pi_{33}(0)$ and $\Pi_{WW}(0)$ from each doublet, hence zero contribution to $\delta\rho$. Thus we conclude that *only diagrams in the third class are relevant to* $\delta\rho$.

Our previous classification and conclusion are very general and go beyond the specific framework we are interested in. Let us now specialize all that to our case. Since we are looking for leading effects in y_t, the Higgs insertions in the third class of diagrams in Fig. 3 should involve $\tilde{t}_L$ or $\tilde{c}_L$, so the external gauge bosons are W^3–W^3. The stop/scharm diagrams that contribute to the ρ parameter at $\mathcal{O}(y_t^4)$ are shown in Fig. 4. Apart from the first diagram, the other ones are related to most of those in Fig. 1, namely, those where two external W^3 bosons can be attached to two *distinct* $\tilde{q}_L$ propagators. The first diagram in Fig. 4 gives a positive contribution to $\delta\rho$. The other ones in the first (second) row are quadratic (quartic) in trilinear couplings and give negative (positive) contributions. The result of our computation is:

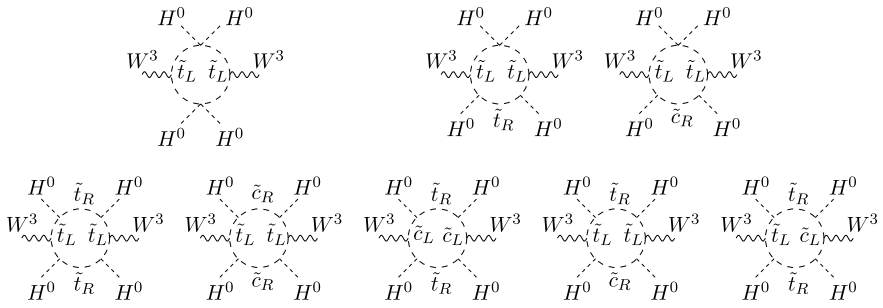

Fig. 4. One-loop stop/scharm diagrams that contribute to the ρ parameter at $\mathcal{O}(y_t^4)$.

$$
\begin{aligned}
\delta\rho = \frac{3y_t^4}{16\pi^2}\frac{v^2}{\tilde m_{t_L}^2}\Bigg\{ & \frac{1}{6} - \frac{|X_t|^2}{\tilde m_{t_R}^2} g_1\left(\frac{\tilde m_{t_L}^2}{\tilde m_{t_R}^2}\right) - \frac{|A_{ct}|^2}{\tilde m_{c_R}^2} g_1\left(\frac{\tilde m_{t_L}^2}{\tilde m_{c_R}^2}\right) \\
& + \frac{|X_t|^4}{\tilde m_{t_R}^4} g_2\left(\frac{\tilde m_{t_L}^2}{\tilde m_{t_R}^2}\right) + \frac{|A_{ct}|^4}{\tilde m_{c_R}^4} g_2\left(\frac{\tilde m_{t_L}^2}{\tilde m_{c_R}^2}\right) + \frac{|A_{tc}|^4}{\tilde m_{c_L}^4}\cdot\frac{\tilde m_{t_L}^2}{\tilde m_{c_L}^2} g_2\left(\frac{\tilde m_{t_R}^2}{\tilde m_{c_L}^2}\right) \\
& + \frac{|X_t|^2|A_{ct}|^2}{\tilde m_{c_R}^2 - \tilde m_{t_R}^2}\left[\frac{1}{\tilde m_{t_R}^2} g_1\left(\frac{\tilde m_{t_L}^2}{\tilde m_{t_R}^2}\right) - \frac{1}{\tilde m_{c_R}^2} g_1\left(\frac{\tilde m_{t_L}^2}{\tilde m_{c_R}^2}\right)\right] \\
& + 2\frac{|X_t|^2|A_{tc}|^2}{(\tilde m_{c_L}^2 - \tilde m_{t_L}^2)^2}\Bigg[f_3\left(\frac{\tilde m_{t_R}^2}{\tilde m_{t_L}^2}\right) + \frac{\tilde m_{t_L}^2}{\tilde m_{c_L}^2} f_3\left(\frac{\tilde m_{t_R}^2}{\tilde m_{c_L}^2}\right) \\
& + \frac{\tilde m_{t_L}^2}{\tilde m_{c_L}^2 - \tilde m_{t_L}^2}\left(f_1\left(\frac{\tilde m_{t_R}^2}{\tilde m_{t_L}^2}\right) - f_1\left(\frac{\tilde m_{t_R}^2}{\tilde m_{c_L}^2}\right)\right)\Bigg]\Bigg\},
\end{aligned}
\tag{8}
$$

where $f_1(x)$ and $f_3(x)$ have been defined in eqs. (4) and (6), and $g_i(x)$ are other positive functions [with $g_1(0) = \frac{1}{3}$, $g_1(1) = \frac{1}{12}$, $g_2(0) = \frac{1}{6}$, $g_2(1) = \frac{1}{60}$]:

$$
g_1(x) = \frac{x}{(x-1)^4}\log x + \frac{x^2 - 5x - 2}{6(x-1)^3}, \quad g_2(x) = -\frac{x(x+1)}{(x-1)^5}\log x + \frac{x^2 + 10x + 1}{6(x-1)^4}. \tag{9}
$$

The structure of eq. (8) resembles that of Δ in eq. (3). Flavour conserving and flavour changing trilinears appear on the same footing and can give effects of the same order. At variance with Δ, though, $\delta\rho$ is not left–right symmetric and is suppressed by an overall factor $v^2/\tilde m_{t_L}^2$. All such features are expected, of course. In the simplified scenario where $\tilde m_{t_L}^2 \simeq \tilde m_{t_R}^2 \simeq \tilde m_t^2$ and $\tilde m_{c_L}^2 \simeq \tilde m_{c_R}^2 \simeq \tilde m_c^2$, the above result reads:

$$
\begin{aligned}
\delta\rho = \frac{3y_t^4}{16\pi^2}\frac{v^2}{\tilde m_t^2}\Bigg\{ & \frac{1}{6} - \frac{1}{12}\frac{|X_t|^2}{\tilde m_t^2} - \frac{|A_{ct}|^2}{\tilde m_c^2} g_1\left(\frac{\tilde m_t^2}{\tilde m_c^2}\right) \\
& + \frac{1}{60}\frac{|X_t|^4}{\tilde m_t^4} + \left(\frac{|A_{ct}|^4}{\tilde m_c^4} + \frac{|A_{tc}|^4}{\tilde m_c^4}\cdot\frac{\tilde m_t^2}{\tilde m_c^2}\right) g_2\left(\frac{\tilde m_t^2}{\tilde m_c^2}\right) \\
& + \frac{|X_t|^2}{\tilde m_t^2}\left[\frac{|A_{ct}|^2}{\tilde m_c^2} g_3\left(\frac{\tilde m_t^2}{\tilde m_c^2}\right) + 2\frac{|A_{tc}|^2}{\tilde m_c^2}\cdot\frac{\tilde m_t^2}{\tilde m_c^2} g_2\left(\frac{\tilde m_t^2}{\tilde m_c^2}\right)\right]\Bigg\},
\end{aligned}
\tag{10}
$$

where $g_3(x)$ is another positive function [with $g_3(0) = \frac{1}{12}$, $g_3(1) = \frac{1}{30}$]:

$$g_3(x) = \frac{x^2}{(x-1)^5}\log x + \frac{x^3 - 7x^2 - 7x + 1}{12(x-1)^4}\,. \tag{11}$$

In the flavour conserving limit ($A_{tc} = A_{ct} = 0$), eq. (10) reduces to

$$\delta\rho|_{\text{fl.cons.}} = \frac{y_t^4}{32\pi^2}\frac{v^2}{\tilde{m}_t^2}\left[1 - \frac{1}{2}\frac{|X_t|^2}{\tilde{m}_t^2} + \frac{1}{10}\frac{|X_t|^4}{\tilde{m}_t^4}\right], \tag{12}$$

which is consistent with the first SUSY computation of $\delta\rho$ [19]. The expression of $\delta\rho|_{\text{fl.cons.}}$ for $\tilde{m}_{t_L}^2 \neq \tilde{m}_{t_R}^2$ can be easily read off from eq. (8). Eq. (12) also agrees with one of the results presented in Ref. [22], where the coefficients of several $d = 6$ effective operators were computed, in the flavour conserving case with degenerate stop masses.[2]

Other limits of eq. (10) lead to simple expressions for $\delta\rho$. For instance, in the degenerate limit ($\tilde{m}_c^2 = \tilde{m}_t^2 = \tilde{m}^2$) we obtain:

$$\delta\rho = \frac{y_t^4}{32\pi^2}\frac{v^2}{\tilde{m}^2} \times\left[1 - \frac{|X_t|^2 + |A_{ct}|^2}{2\tilde{m}^2} + \frac{|X_t|^4 + |A_{tc}|^4 + |A_{ct}|^4 + 2|X_t|^2(|A_{tc}|^2 + |A_{ct}|^2)}{10\tilde{m}^4}\right]. \tag{13}$$

The expression in brackets, which resembles Δ in eq. (7), is positive and generically $\mathcal{O}(1)$. More precisely, its value is 1 at vanishing trilinears, minimal ($= \frac{3}{8}$) at $|X_t|^2 + |A_{ct}|^2 = \frac{5}{2}\tilde{m}^2$ (with $|A_{tc}| = 0$), and large ($\gg 1$) if any of the trilinears is much larger than $\tilde{m}$. Barring the latter case, we can see that $\delta\rho$ is sufficiently suppressed even for light squark masses (the prefactor $y_t^4 v^2/(32\pi^2\tilde{m}^2)$ is about $2 \cdot 10^{-4}$ for $\tilde{m} \sim 500$ GeV, if one takes $y_t^4 \sim 0.6$ at that scale). On the other hand, either eq. (13) or the more general expressions presented above, eqs. (8) and (10), could be useful in case future electroweak precision measurements should require a small non-vanishing $\delta\rho$.

Another interesting expression can be obtained from eq. (10) in the hierarchical limit ($\tilde{m}_c^2 \gg \tilde{m}_t^2$):

$$\delta\rho \simeq \frac{y_t^4}{32\pi^2}\frac{v^2}{\tilde{m}_t^2}\left[\left(1 - \frac{|A_{ct}|^2}{\tilde{m}_c^2}\right)^2 - \frac{1}{2}\frac{|X_t|^2}{\tilde{m}_t^2}\left(1 - \frac{|A_{ct}|^2}{\tilde{m}_c^2}\right) + \frac{1}{10}\frac{|X_t|^4}{\tilde{m}_t^4}\right]. \tag{14}$$

Here flavour violating parameters only appear through $|A_{ct}|^2/\tilde{m}_c^2$, which should be actually interpreted as $|A_{ct}|^2/\tilde{m}_{c_R}^2$. Terms dependent on $|A_{tc}|^2$ and $\tilde{m}_{c_L}^2$ are suppressed by $\tilde{m}_t^2/\tilde{m}_{c_L}^2$ and are not shown. The previous expression is consistent with the result one obtains by first decoupling $\tilde{c}_R$ and then computing $\delta\rho$. In this approach, the trilinear couplings $y_t A_{ct} H^0 \tilde{c}_R^* \tilde{t}_L + \text{h.c.}$ and the tree-level exchange of $\tilde{c}_R$ generate an effective quartic interaction of the same form $|H^0|^2|\tilde{t}_L|^2$ as the

[2] In Ref. [22] subleading terms of order $g^2 y_t^2$ and g^4 have been evaluated as well. We confirm those terms, which we have obtained by including D-term contributions to both $\Pi_{33}(0)$ and $\Pi_{WW}(0)$, again by considering diagrams of the third class in Fig. 3, with up-type and down-type squark propagators. In fact, we have found that even our general result for $\delta\rho$ in eq. (8) can easily be extended to account for all D-term effects, also including squarks and sleptons of all generations. The recipe is: *i)* in the term without trilinears, replace $3y_t^4/\tilde{m}_{t_L}^2$ by $3(y_t^2 + \cos 2\beta\, g^2/2)^2/\tilde{m}_{t_L}^2 + (\cos 2\beta\, g^2/2)^2(3/\tilde{m}_{c_L}^2 + 3/\tilde{m}_{u_L}^2 + 1/\tilde{m}_{e_L}^2 + 1/\tilde{m}_{\mu_L}^2 + 1/\tilde{m}_{\tau_L}^2)$; *ii)* in the terms proportional to $|X_t|^2$ and $|A_{ct}|^2$, replace y_t^4 by $y_t^2(y_t^2 + \cos 2\beta\, g^2/2)$; *iii)* add the term $-v^2/(16\pi^2) \cdot (3y_t^2 \cos 2\beta\, g^2/2)|A_{tc}|^2/(\tilde{m}_{c_L}^2 \tilde{m}_{t_R}^2) \cdot g_1(\tilde{m}_{c_L}^2/\tilde{m}_{t_R}^2)$.

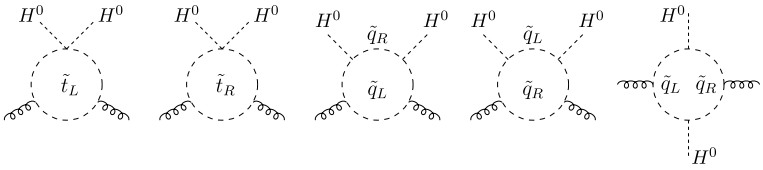

Fig. 5. One-loop stop/scharm diagrams that contribute to the effective Higgs coupling to gluons or photons at $\mathcal{O}(y_t^2)$ ($\tilde{q}_L \in \{\tilde{t}_L, \tilde{c}_L\}$, $\tilde{q}_R \in \{\tilde{t}_R, \tilde{c}_R\}$).

SUSY one, such that the overall effective coupling is $\xi y_t^2 |H^0|^2 |\tilde{t}_L|^2$, where $\xi \equiv 1 - |A_{ct}|^2/\tilde{m}_{c_R}^2$. Therefore one can take the expression of $\delta\rho$ in the flavour conserving case, eq. (12), rescale the first term by ξ^2 and the second one by ξ, since they originate from diagrams with either two or one insertion(s) of $|H^0|^2|\tilde{t}_L|^2$, respectively. In this way eq. (14) is recovered. As far as the size of $\delta\rho$ is concerned, we can notice again that eq. (14) exhibits a suppression factor, controlled by $v^2/\tilde{m}_t^2$, times an $\mathcal{O}(1)$ factor, *i.e.*, the expression in square brackets. The latter one is positive except at $|A_{ct}|^2 = \tilde{m}_c^2$ and $X_t = 0$, where it vanishes, so $\delta\rho$ is further suppressed in a neighbourhood of that point. Notice that scharm effects are significant even for $\tilde{m}_c^2 \gg \tilde{m}_t^2$, provided $|A_{ct}|^2 = \mathcal{O}(\tilde{m}_c^2)$.

4. The processes $gg \leftrightarrow h$ and $h \to \gamma\gamma$

After the previous digression on the ρ parameter, we now return to discuss properties of the physical Higgs boson h, namely its effective couplings with other SM particles. Such couplings can be parametrized through phenomenological scale factors κ_i [23], which encode possible deviations from the SM predictions. In particular, κ_g and κ_γ are associated with crucial processes such as $gg \leftrightarrow h$ and $h \to \gamma\gamma$:

$$\frac{\sigma(gg \to h)}{\sigma^{\rm SM}(gg \to h)} \simeq \frac{\Gamma(h \to gg)}{\Gamma^{\rm SM}(h \to gg)} = \kappa_g^2, \qquad \frac{\Gamma(h \to \gamma\gamma)}{\Gamma^{\rm SM}(h \to \gamma\gamma)} = \kappa_\gamma^2 \,. \tag{15}$$

We can write $\kappa_g = 1 + \delta\kappa_g$ and $\kappa_\gamma = 1 + \delta\kappa_\gamma$, where $\delta\kappa_g$ and $\delta\kappa_\gamma$ encode the corrections from new physics, normalized to the SM amplitudes ($\delta\kappa_g = \delta\mathcal{A}_{hgg}/\mathcal{A}_{hgg}^{\rm SM}$, $\delta\kappa_\gamma = \delta\mathcal{A}_{h\gamma\gamma}/\mathcal{A}_{h\gamma\gamma}^{\rm SM}$). In our scenario and within our assumptions, $\delta\kappa_g$ and $\delta\kappa_\gamma$ are proportional to $v^2/\tilde{m}^2$ and are related to the $d = 6$ operators $|H^0|^2 G_{\mu\nu} G^{\mu\nu}$ and $|H^0|^2 F_{\mu\nu} F^{\mu\nu}$, which receive $\mathcal{O}(y_t^2)$ contributions from the one-loop stop/scharm diagrams shown in Fig. 5. Let us consider first the case of external gluons. We have computed those diagrams at vanishing Higgs momenta and kept terms quadratic in the gluon momenta (the terms at zero gluon momenta are canceled by other diagrams with quartic gluon–squark couplings, consistently with gauge invariance). By comparing with the SM result, which is dominated by a top loop, we find:

$$\delta\kappa_g \simeq \frac{m_t^2}{4}\left[\frac{1}{\tilde{m}_{t_L}^2}\left(1 - \frac{|A_{ct}|^2}{\tilde{m}_{c_R}^2}\right) + \frac{1}{\tilde{m}_{t_R}^2}\left(1 - \frac{|A_{tc}|^2}{\tilde{m}_{c_L}^2}\right) - \frac{|X_t|^2}{\tilde{m}_{t_L}^2 \tilde{m}_{t_R}^2}\right] . \tag{16}$$

We have also checked that the same expression can be derived through Higgs low-energy theorems [24]. Indeed, the one-loop correction to the coefficient of $G_{\mu\nu}G^{\mu\nu}$ induced by stop and scharm squarks in a Higgs background is proportional to $b \log\det \mathcal{M}^2$, where b is the appropriate β-function coefficient and $\mathcal{M}^2 = \mathcal{M}^2(H^0)$ is the (4×4) Higgs-dependent squark mass matrix. Therefore, by expanding $\log\det\mathcal{M}^2$ up to $\mathcal{O}(|H^0|^2)$, we have found the coupling of interest and recovered eq. (16) after normalizing to the top contribution. Our result for $\delta\kappa_g$ generalizes

the well studied one without flavour violation (see, *e.g.*, [25,6,26,22]). The effect of the novel terms proportional to $|A_{ct}|^2$ and $|A_{tc}|^2$ is analogous to that of $|X_t|^2$, *i.e.*, all trilinear parameters generate negative contributions to $\delta\kappa_g$, which can therefore have either sign. Although eq. (16) is already very simple, for completeness we also write $\delta\kappa_g$ in the simplified scenario where $\tilde{m}^2_{t_L} \simeq \tilde{m}^2_{t_R} \simeq \tilde{m}^2_t$ and $\tilde{m}^2_{c_L} \simeq \tilde{m}^2_{c_R} \simeq \tilde{m}^2_c$:

$$\delta\kappa_g \simeq \frac{m_t^2}{2\tilde{m}_t^2}\left[1 - \frac{1}{2}\left(\frac{|X_t|^2}{\tilde{m}_t^2} + \frac{|A_{ct}|^2 + |A_{tc}|^2}{\tilde{m}_c^2}\right)\right]. \tag{17}$$

Notice that for $\tilde{m}_c^2 \gtrsim \tilde{m}_t^2$ the size of $\delta\kappa_g$ is controlled by $m_t^2/\tilde{m}_t^2$, yet the effects of scharm squarks are not sub-leading even in the hierarchical limit ($\tilde{m}_c^2 \gg \tilde{m}_t^2$), provided $|A_{tc}|^2$ and/or $|A_{ct}|^2$ are of order $\tilde{m}_c^2$. An analogous comment applies to the general result of eq. (16). Finally, in the degenerate limit ($\tilde{m}_c^2 = \tilde{m}_t^2 = \tilde{m}^2$) the previous result becomes:

$$\delta\kappa_g \simeq \frac{m_t^2}{2\tilde{m}^2}\left[1 - \frac{|X_t|^2 + |A_{ct}|^2 + |A_{tc}|^2}{2\tilde{m}^2}\right]. \tag{18}$$

The computation of the squark contribution to the Higgs-photon coupling is completely analogous to that of the Higgs-gluon coupling. The main change is the normalization to the SM amplitude, where the leading one-loop effect comes from W's whilst the top loop generates a smaller contribution of opposite sign. In practice, since $\mathcal{A}^{\rm top}_{h\gamma\gamma} \simeq -0.3\,\mathcal{A}^{\rm SM}_{h\gamma\gamma}$, one gets $\delta\kappa_\gamma \simeq -0.3\,\delta\kappa_g$.

The latter (anti)correlation between $\delta\kappa_\gamma$ and $\delta\kappa_g$ holds when other SUSY contributions to $\delta\kappa_\gamma$ are negligible. That relation is useful also because LHC results on Higgs physics are sometimes presented as confidence regions in the plane $(\kappa_\gamma, \kappa_g)$, under the assumption that other Higgs couplings are SM-like. Therefore we can intersect the line $\delta\kappa_\gamma = -0.3\,\delta\kappa_g$ with the 95% C.L. contours reported by either CMS [3] or ATLAS [4] and infer bounds such as $-0.3 \lesssim \delta\kappa_g \lesssim 0.15$ or $-0.15 \lesssim \delta\kappa_g \lesssim 0.45$, respectively. These ranges translate into constraints on the combination of masses and trilinear couplings (both flavour conserving and flavour changing ones) that appear either in eq. (16) or in its simplified versions, eqs. (17) and (18). In analogy to our discussion on $\delta\rho$, we can see that bounds are not very restrictive at present, but will be important when κ_g and κ_γ are measured more precisely, first at the LHC and then at future colliders. Thus the processes $gg \leftrightarrow h$ and $h \to \gamma\gamma$ can be sensitive probes not only of stop parameters [25,6,26,22], but also, more generally, of the full stop/scharm sector.[3]

5. The decay $h \to c\bar{c}$

In the previous section we have discussed Higgs couplings to gluons or photons, where the leading SM amplitudes arise at the one-loop level. SUSY corrections are potentially important because they contribute at the same perturbative order and are only suppressed by the usual decoupling factor $v^2/\tilde{m}^2$, relatively to the SM. The case of Higgs couplings to fermions has both similarities and differences with the previous one. In fact, in the SM, Yukawa couplings are present at the tree level, but they are suppressed for light fermions because they are proportional to fermion masses. Therefore loop corrections from new physics can be important if they do not respect that proportionality. In the special framework discussed in our paper, such a situation

[3] We also recall that even direct searches for stops are affected by the presence of A_{tc} and/or A_{ct}. For instance, since these parameters induce stop/scharm mass mixing, decays such as $\tilde{t}_i \to c\tilde{\chi}^0$ can proceed at the tree level.

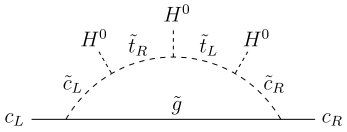

Fig. 6. One-loop stop/scharm/gluino contribution to the effective Higgs coupling to charm quarks.

arises for the charm quark provided all three trilinears (X_t, A_{tc} and A_{ct}) are simultaneously present and unsuppressed.

Before presenting our computation, let us recall again the phenomenological κ_i parametrization [23], which in the case of the decay $h \to c\bar{c}$ reads as

$$\frac{\Gamma(h \to c\bar{c})}{\Gamma^{\rm SM}(h \to c\bar{c})} = \kappa_c^2 \simeq 1 + 2\,\delta\kappa_c\,, \tag{19}$$

where we have expanded $\kappa_c = 1 + \delta\kappa_c$ and $\delta\kappa_c = \mathcal{O}(v^2/\tilde{m}^2)$ encodes the corrections from new physics. At the Lagrangian level, using the previous expression amounts to parametrize the mass of the charm quark and its effective coupling to the physical Higgs boson h as

$$\mathcal{L}_c = -m_c \left(1 + \kappa_c \frac{h}{\sqrt{2}v}\right) \bar{c}c\,. \tag{20}$$

In terms of the Higgs field H^0, the SM limit ($\kappa_c = 1$) is described by the $d = 4$ Yukawa operator $-(y_c H^0 \overline{c_R} c_L + \text{h.c.})$, whereas the leading effects of non-SM physics are associated with the $d = 6$ effective operator $C_c |H^0|^2 H^0 \overline{c_R} c_L + \text{h.c.}$ [27], which we treat as a small perturbation.[4] The latter contributes to the charm mass and to the Higgs-charm coupling with different numerical coefficients, *i.e.* $\delta m_c = -(\text{Re}\, C_c)\, v^3$ and $\delta(\kappa_c m_c) = -3\,(\text{Re}\, C_c)\, v^3$, so the physically relevant correction is $\delta\kappa_c = -2\,(\text{Re}\, C_c)\, v^3/m_c$. In our scenario, the dominant contribution to that $d = 6$ effective operator is generated by the one-loop stop/scharm/gluino diagram shown in Fig. 6. A crucial feature of such a diagram is that the chiral transition from c_L to c_R does not involve the charm Yukawa coupling, since it occurs through three chirality flips associated with the trilinear couplings X_t, A_{tc}, A_{ct}. We obtain:

$$\delta\kappa_c = -\frac{4\alpha_s}{3\pi} \left(\frac{m_t}{m_c}\right) m_t^2\, \text{Re}(A_{ct} X_t^* A_{tc} M_g^*) \cdot I\,(|M_g|^2, \tilde{m}^2_{c_L}, \tilde{m}^2_{c_R}, \tilde{m}^2_{t_L}, \tilde{m}^2_{t_R})\,, \tag{21}$$

where M_g is the gluino mass and I is the five-point loop function:

$$I(a,b,c,d,e) = \frac{b\log(b/a)}{(b-a)(b-c)(b-d)(b-e)} + (b \leftrightarrow c) + (b \leftrightarrow d) + (b \leftrightarrow e)\,. \tag{22}$$

The simplified scenario in which $\tilde{m}^2_{t_L} \simeq \tilde{m}^2_{t_R}$ and $\tilde{m}^2_{c_L} \simeq \tilde{m}^2_{c_R}$ is described by the following limit of eq. (22):

$$I(a,b,b,c,c) = \frac{1}{a(b-c)^2}\left[f_1\left(\frac{b}{a}\right) + f_1\left(\frac{c}{a}\right) - \frac{2a}{b-c}\left(\frac{b\log(b/a)}{b-a} - \frac{c\log(c/a)}{c-a}\right)\right], \tag{23}$$

[4] This is justified *a posteriori*. Also, we consider a field basis in which y_c is real and neglect the effect of $\text{Im}\, C_c$, which induces a CP violating coupling of h to $i\bar{c}\gamma_5 c$ and corrects the ratio in eq. (19) at $\mathcal{O}(v^4/\tilde{m}^4)$.

where $f_1(x)$ has been defined in eq. (4). Eq. (23) can also be used in a scenario with $\tilde{m}^2_{t_L} \simeq \tilde{m}^2_{c_L}$ and $\tilde{m}^2_{t_R} \simeq \tilde{m}^2_{c_R}$, because $I(a,b,c,b,c) = I(a,b,b,c,c)$. Finally, in the degenerate limit in which all stop and scharm squarks have a common mass $\tilde{m}^2$, the result reads:

$$\delta\kappa_c = -\frac{4\alpha_s}{3\pi}\left(\frac{m_t}{m_c}\right)\left(\frac{m_t^2}{\tilde{m}^2}\right)\left[\frac{\mathrm{Re}(A_{ct}X_t^* A_{tc} M_g^*)}{\tilde{m}^4}\, g_1\left(\frac{|M_g|^2}{\tilde{m}^2}\right)\right], \tag{24}$$

where $g_1(x)$ has been defined in eq. (9) [note that $g_1(|M_g|^2/\tilde{m}^2) \to 1/12$ when $|M_g|^2 \to \tilde{m}^2$].

The main properties of the correction $\delta\kappa_c$ are manifest both in our general result, eq. (21), and in its simplified version, eq. (24). Consider the latter expression. One can notice that the loop factor and the decoupling factor $m_t^2/\tilde{m}^2$, which suppress $\delta\kappa_c$, are partly compensated by the large enhancement factor m_t/m_c, whose value is about $2.7 \cdot 10^2$ at the weak or SUSY scale. The expression in square brackets is a dimensionless function of SUSY mass parameters. The general case is described by eq. (21). As a numerical example, suppose that the gluino, stop and scharm masses as well as the three trilinear parameters have a common size of about 1 TeV. Then $\delta\kappa_c \sim \pm 3 \cdot 10^{-2}$, which implies a 6% deviation of $\Gamma(h \to c\bar{c})$ with respect to the SM prediction. However, it is clear that even moderate variations around that parameter point can generate very different results. For instance, increasing all trilinear parameters to 1.5 TeV while keeping squark and gluino masses at 1 TeV would lead to a sizable 20% deviation in $\Gamma(h \to c\bar{c})$, while a similar change with reversed roles would reduce the deviation to 1% only. Splitting squark masses can produce further variations.[5]

As a final comment, we recall that the sensitivity of $\Gamma(h \to c\bar{c})$ to flavour violation in the stop/scharm sector of the MSSM has been recently pointed out and explored in [28]. Flavour violating terms of all types (LL, RR, LR) have been considered and potentially large effects have been reported. In our study we have focused on LR flavour violation, used a simpler computational method and obtained simpler analytical expressions, which expose the relevant parametric dependences. Although a quantitative comparison between our results and those in [28] is not straightforward, we have noticed that the effects reported there are typically larger than those we find, even if we extend our approach to include LL and RR violation. We do not have an explanation for such a discrepancy. At the qualitative level, though, we confirm the potential relevance of SUSY flavour violation to the decay $h \to c\bar{c}$ and agree with the conclusion in [28] that such effects may be tested at a future e^+e^- collider through precision measurements, while that task will be hard at the LHC because of the difficulties in charm tagging.[6]

6. Conclusions

After the discovery of the Higgs boson at the LHC, many efforts will be devoted to measure its couplings more precisely and to look for possible deviations from the SM expectations. At the

[5] The above corrections to the Higgs-charm effective coupling could be compared with different ones, which arise from integrating out the heavy Higgs doublet. In the MSSM, for instance, one obtains a tree-level contribution to the $|H^0|^2 H^0 \overline{c_R} c_L$ effective operator such that $\delta\kappa_c \simeq 2\cos 2\beta \cos^2\beta \cdot m_Z^2/m_A^2$, where m_A is the heavy Higgs mass. This correction is negative and its size is smaller than 10^{-2} for $m_A \gtrsim 500$ GeV.

[6] For recent studies on the observability of the Higgs-charm coupling, see also [29] and refs. therein. Regarding other interesting processes that involve the Higgs boson and charm quarks, we recall that A_{tc} or A_{ct} can also induce the decay $t \to ch$ through one-loop diagrams. According to [30], however, the associated branching ratio can hardly exceed $\mathcal{O}(10^{-6})$, which is below the LHC sensitivity.

same time, the search for new particles will continue and higher mass ranges will be probed. The framework beyond the SM that we have examined in this paper is a SUSY scenario with large flavour violating A-terms in the stop/scharm sector. By integrating out stop and scharm squarks at the one-loop level, we have computed the leading corrections induced by A_{tc} and A_{ct} on the Higgs mass, the electroweak ρ parameter and the effective Higgs couplings to gluons, photons and charm quarks. For each of such quantities we have presented explicit analytical expressions which exhibit the relevant parametric dependences, both in the general case and in special limits. In particular, by treating A_{tc} and A_{ct} on the same footing as the flavour conserving parameter X_t, we have emphasized that all three trilinear couplings play similar roles and can induce significant effects. We have also checked that each of the above observables has the correct scaling behaviour under the decoupling of SUSY particles, as expected from the dimensionality ($d = 4$ or $d = 6$) of the associated effective operators, and have discussed some phenomenological implications at the LHC and future colliders. It is also clear that the importance of the indirect SUSY effects investigated in this paper is both related and complementary to the results of ongoing direct searches of SUSY particles.

Acknowledgements

We thank P. Paradisi for discussions.

References

[1] S. Chatrchyan, et al., CMS Collaboration, Phys. Lett. B 716 (2012) 30, arXiv:1207.7235 [hep-ex];
G. Aad, et al., ATLAS Collaboration, Phys. Lett. B 716 (2012) 1, arXiv:1207.7214 [hep-ex].
[2] G. Aad, et al., ATLAS Collaboration, CMS Collaboration, Phys. Rev. Lett. 114 (2015) 191803, arXiv:1503.07589 [hep-ex].
[3] V. Khachatryan, et al., CMS Collaboration, Eur. Phys. J. C 75 (5) (2015) 212, arXiv:1412.8662 [hep-ex].
[4] ATLAS Collaboration, ATLAS-CONF-2015-007.
[5] H.P. Nilles, Phys. Rep. 110 (1984) 1;
H.E. Haber, G.L. Kane, Phys. Rep. 117 (1985) 75;
S.P. Martin, Adv. Ser. Dir. High Energy Phys. 21 (2010) 1, arXiv:hep-ph/9709356.
[6] A. Djouadi, Phys. Rep. 459 (2008) 1, arXiv:hep-ph/0503173.
[7] M. Drees, Int. J. Mod. Phys. A 4 (1989) 3635;
J.R. Ellis, J.F. Gunion, H.E. Haber, L. Roszkowski, F. Zwirner, Phys. Rev. D 39 (1989) 844;
U. Ellwanger, C. Hugonie, A.M. Teixeira, Phys. Rep. 496 (2010) 1, arXiv:0910.1785 [hep-ph].
[8] A. Brignole, P. Paradisi, in preparation.
[9] A. Strumia, Phys. Lett. B 466 (1999) 107, arXiv:hep-ph/9906266;
N. Polonsky, S. Su, Phys. Lett. B 508 (2001) 103, arXiv:hep-ph/0010113;
A. Brignole, J.A. Casas, J.R. Espinosa, I. Navarro, Nucl. Phys. B 666 (2003) 105, arXiv:hep-ph/0301121;
M. Dine, N. Seiberg, S. Thomas, Phys. Rev. D 76 (2007) 095004, arXiv:0707.0005 [hep-ph];
I. Antoniadis, E. Dudas, D.M. Ghilencea, P. Tziveloglou, Nucl. Phys. B 808 (2009) 155, arXiv:0806.3778 [hep-ph];
I. Antoniadis, E. Dudas, D.M. Ghilencea, P. Tziveloglou, Nucl. Phys. B 831 (2010) 133, arXiv:0910.1100 [hep-ph].
[10] Y. Okada, M. Yamaguchi, T. Yanagida, Prog. Theor. Phys. 85 (1991) 1;
Y. Okada, M. Yamaguchi, T. Yanagida, Phys. Lett. B 262 (1991) 54;
J.R. Ellis, G. Ridolfi, F. Zwirner, Phys. Lett. B 257 (1991) 83;
J.R. Ellis, G. Ridolfi, F. Zwirner, Phys. Lett. B 262 (1991) 477;
H.E. Haber, R. Hempfling, Phys. Rev. Lett. 66 (1991) 1815;
H.E. Haber, R. Hempfling, Phys. Rev. D 48 (1993) 4280, arXiv:hep-ph/9307201;
R. Barbieri, M. Frigeni, F. Caravaglios, Phys. Lett. B 258 (1991) 167;
J.R. Espinosa, M. Quiros, Phys. Lett. B 266 (1991) 389;
P.H. Chankowski, S. Pokorski, J. Rosiek, Phys. Lett. B 274 (1992) 191;
A. Brignole, Phys. Lett. B 281 (1992) 284.

[11] E. Bagnaschi, G.F. Giudice, P. Slavich, A. Strumia, J. High Energy Phys. 1409 (2014) 092, arXiv:1407.4081 [hep-ph].
[12] H.E. Haber, R. Hempfling, A.H. Hoang, Z. Phys. C 75 (1997) 539, arXiv:hep-ph/9609331.
[13] J.M. Frere, D.R.T. Jones, S. Raby, Nucl. Phys. B 222 (1983) 11;
L. Alvarez-Gaume, J. Polchinski, M.B. Wise, Nucl. Phys. B 221 (1983) 495.
[14] J.A. Casas, S. Dimopoulos, Phys. Lett. B 387 (1996) 107, arXiv:hep-ph/9606237;
J.h. Park, Phys. Rev. D 83 (2011) 055015, arXiv:1011.4939 [hep-ph].
[15] J. Cao, G. Eilam, K.i. Hikasa, J.M. Yang, Phys. Rev. D 74 (2006) 031701, arXiv:hep-ph/0604163.
[16] M. Arana-Catania, S. Heinemeyer, M.J. Herrero, S. Penaranda, J. High Energy Phys. 1205 (2012) 015, arXiv:1109.6232 [hep-ph];
M. Arana-Catania, S. Heinemeyer, M.J. Herrero, S. Penaranda, Phys. Rev. D 90 (7) (2014) 075003, arXiv:1405.6960 [hep-ph].
[17] K. Kowalska, J. High Energy Phys. 1409 (2014) 139, arXiv:1406.0710 [hep-ph].
[18] M. Baak, et al., Gfitter Group Collaboration, Eur. Phys. J. C 74 (2014) 3046, arXiv:1407.3792 [hep-ph].
[19] R. Barbieri, L. Maiani, Nucl. Phys. B 224 (1983) 32.
[20] C.S. Lim, T. Inami, N. Sakai, Phys. Rev. D 29 (1984) 1488;
M. Drees, K. Hagiwara, Phys. Rev. D 42 (1990) 1709.
[21] S. Heinemeyer, W. Hollik, F. Merz, S. Penaranda, Eur. Phys. J. C 37 (2004) 481, arXiv:hep-ph/0403228;
S. Heinemeyer, W. Hollik, G. Weiglein, Phys. Rep. 425 (2006) 265, arXiv:hep-ph/0412214.
[22] B. Henning, X. Lu, H. Murayama, arXiv:1404.1058 [hep-ph];
B. Henning, X. Lu, H. Murayama, arXiv:1412.1837 [hep-ph].
[23] A. David, et al., LHC Higgs Cross Section Working Group Collaboration, arXiv:1209.0040 [hep-ph].
[24] J.R. Ellis, M.K. Gaillard, D.V. Nanopoulos, Nucl. Phys. B 106 (1976) 292;
M.A. Shifman, A.I. Vainshtein, M.B. Voloshin, V.I. Zakharov, Sov. J. Nucl. Phys. 30 (1979) 711, Yad. Fiz. 30 (1979) 1368.
[25] A. Djouadi, Phys. Lett. B 435 (1998) 101, arXiv:hep-ph/9806315.
[26] K. Blum, R.T. D'Agnolo, J. Fan, J. High Energy Phys. 1301 (2013) 057, arXiv:1206.5303 [hep-ph];
M.R. Buckley, D. Hooper, Phys. Rev. D 86 (2012) 075008, arXiv:1207.1445 [hep-ph];
J.R. Espinosa, C. Grojean, V. Sanz, M. Trott, J. High Energy Phys. 1212 (2012) 077, arXiv:1207.7355 [hep-ph];
A. Delgado, G.F. Giudice, G. Isidori, M. Pierini, A. Strumia, Eur. Phys. J. C 73 (3) (2013) 2370, arXiv:1212.6847 [hep-ph];
M. Carena, S. Gori, N.R. Shah, C.E.M. Wagner, L.T. Wang, J. High Energy Phys. 1308 (2013) 087, arXiv:1303.4414 [hep-ph];
J. Fan, M. Reece, J. High Energy Phys. 1406 (2014) 031, arXiv:1401.7671 [hep-ph];
J. Fan, M. Reece, L.T. Wang, arXiv:1412.3107 [hep-ph];
A. Drozd, J. Ellis, J. Quevillon, T. You, J. High Energy Phys. 1506 (2015) 028, arXiv:1504.02409 [hep-ph].
[27] W. Buchmuller, D. Wyler, Nucl. Phys. B 268 (1986) 621.
[28] A. Bartl, H. Eberl, E. Ginina, K. Hidaka, W. Majerotto, Phys. Rev. D 91 (1) (2015) 015007, arXiv:1411.2840 [hep-ph].
[29] G. Perez, Y. Soreq, E. Stamou, K. Tobioka, arXiv:1505.06689 [hep-ph].
[30] J. Cao, C. Han, L. Wu, J.M. Yang, M. Zhang, Eur. Phys. J. C 74 (9) (2014) 3058, arXiv:1404.1241 [hep-ph];
A. Dedes, M. Paraskevas, J. Rosiek, K. Suxho, K. Tamvakis, J. High Energy Phys. 1411 (2014) 137, arXiv:1409.6546 [hep-ph].